Theoretical studies of methane adsorption on Silica-Kaolinite interface for shale reservoir application

Abdulmujeeb T. Onawole, Mustafa S. Nasser, Ibnelwaleed A. Hussein, Mohammed J. Al-Marri, Santiago Aparicio

Applied Surface Science 546 (2021) 149164

Contents lists available at ScienceDirect

Applied Surface Science

journal homepage: www.elsevier.com/locate/apsusc

Full Length Article

Theoretical studies of methane adsorption on Silica-Kaolinite interface for shale reservoir application

Abdulmujeeb T. Onawole [a], Mustafa S. Nasser [a,*], Ibnelwaleed A. Hussein [a,*], Mohammed J. Al-Marri [b], Santiago Aparicio [c]

[a] Gas Processing Center, College of Engineering, PO Box 2713, Qatar University, Doha, Qatar
[b] Chemical Engineering Department, College of Engineering, PO Box 2713, Qatar University, Doha, Qatar
[c] Department of Chemistry, University of Burgos, 09001 Burgos, Spain

ARTICLE INFO

Keywords:
Methane
DFT
Silica
Kaolinite
Interface
Shale

ABSTRACT

Shale gas is mostly made up of methane and is currently being exploited in fulfilling the world's energy demands. Density Functional Theory (DFT) and Molecular Dynamics (MD) techniques are employed for understanding methane transport in the pores at typical reservoir conditions. Shale, which is made up of clay and quartz-like material, is represented in this study by a combined silica-kaolinite surface. The simulations revealed that the interface is formed by a chemical bond between silicon to two oxygen atoms from the kaolinite surface. Physisorption is the mode of adsorption of methane irrespective of the position of the gas on the interface. However, methane has stronger adsorption on the kaolinite region than the silica region.

1. Introduction

Shale gas which consists of mostly methane (CH_4) is an unconventional fuel [1]. It has recently gained much popularity as a better alternative to fulfilling the world's energy demands as compared to other conventional fuels such as oil and coal due to its low carbon impact [2,3]. This is evident in the commercial development of shale gas in North America (the USA and Canada) [4,5]. Qatar is the world's largest exporter of liquefied natural gas (LNG) [6,7] and hence the development of shale gas exploitation has the potential to revolutionize the gas industry in the region and the world at large. Shale is mainly a mixture of clay materials such as Kaolinite ($Al_2Si_2O_{54}$) and quartz (SiO_2) or silica as it is often called [8,9]. The shale gas is in three different states-free, adsorbed, and dissolved states with the adsorbed state accounting for about 85% of the total [10,11]. Hence, it is quite important to study the adsorption behavior of methane on shale [12]. Moreover, this will help to develop models that can be used to predict the original gas in place (OGIP) which would help in the development of a realistic reservoir model.

Many experimental techniques such as scanning electron microscopy (SEM), energy dispersive X-ray spectrometry (EDS), and X-ray nano-computed tomography (nano CT) have been used to characterize and analyze the shale pore structure, which is important in understanding methane adsorption [13]. However, these techniques involve using sophisticated equipment that is difficult to operate under the high pressure and high temperature (HPHT) conditions of the reservoir. For instance, in Longmaxi formation, shale gas field in China has a temperature of about 330–360 K and a pressure reaching up to 38 MPa [14] whilst in Qatar, the temperature and pressure reach up to 450 K and 50 MPa, respectively [15]. Such HPHT conditions are quite difficult to achieve in the conventional laboratory in studying the transport properties such as density, viscosity, and diffusion coefficient of methane adsorption. Molecular simulation techniques such as Density Functional Theory (DFT), Grand Canonical Monte Carlo (GCMC), and Molecular Dynamics (MD) have the unique advantage of studying these chemical systems at the atomistic scale at such HPHT conditions [16,17]. Previous works have studied the use of molecular simulation in methane adsorption on shale-like systems. Both Zhang, et al [18] and Zhao et al [19] studied the effect of methane adsorption on Kaolinite surface using DFT while Zhao et al, [20] used the GCMC method to study methane and carbon dioxide (CO_2) adsorption on a silica surface. Other notable works have studied methane adsorption and desorption using GCMC and MD techniques for shale gas exploitation albeit using graphene [21,22]and kerogen models [23].

However, while GCMC and MD can handle a large number of atoms, unlike DFT they cannot give accurate descriptions especially for the

* Corresponding authors.
E-mail addresses: m.nasser@qu.edu.qa (M.S. Nasser), ihussein@qu.edu.qa (I.A. Hussein).

https://doi.org/10.1016/j.apsusc.2021.149164
Received 29 December 2020; Received in revised form 24 January 2021; Accepted 26 January 2021
Available online 30 January 2021

mode of adsorption vis-à-vis chemisorption or physisorption. Hence, the best practice is to study the chemical system using DFT before scaling up to either MD or GCMC. Unlike other DFT studies that study the adsorption on a single surface that is either kaolinite or silica alone. This work creates an interface of both silica and kaolinite as that is closer to the reality of modeling shale which is a mixture of clay and silica materials. Though an earlier work had studied kaolinite and silicate surfaces as a representative of shale [9]. Nevertheless, the surfaces were studied separately and not as an interface. The results of this work will provide the bedrock for future molecular simulation work on studying the transport properties (diffusion, density) of methane adsorption in shale and consequently lead to the development of a model that can be used to predict the original gas in place in shale gas reservoirs.

2. Computational methods

VASP (5.4.4.) code [24] was employed for all plane-wave DFT calculations. The revised Generalized Gradient Approximation of Perdew, Burke, and Ernzerhof (PBE-GGA)) [25,26] was used for exchange–correlation energy for all elements. The Projected Augmented Wave (PAW) pseudopotentials were employed [27,28] for the description of the ion–electron interactions. The semi-empirical correction by Grimme (DFT + D3) was included [29,30] to consider the significance of dispersion forces in describing the interface and the generality of the surfaces.

The computed bulk structures of Silica (mp-7000) [31] and Kaolinite (mp- 41152) [32] were retrieved from the materials project database [33] and used as the input structures in creating the interface. The original lattice parameters of bulk kaolinite used in this study were: a = 5.213 Å, b = 7.479 Å, c = 9.052 Å, α = 91.79°, β = 89.73°, and γ = 105°, and for silica: a = b = 5.022 Å, c = 5.511 Å, α = β = 90°, and γ = 120°. The Bulk structures of both silica and kaolinite were optimized with a plane-wave energy cutoff set at 366.6 eV. Thereafter, both surfaces were cleaved at 001 Miller indices as it is the most stable surface for both silica [34] and kaolinite [35]. The interface builder in Quantum ATK virtual Nano lab [36,37] was used to build the interface. Different strains were applied while building the interface and the strain which had the most stable interface (the lowest energy) was used for subsequent calculations [38]. Moreover, Lin et al [23] had suggested that compressive strain had a positive effect on the adsorption capacity of a surface. Hence, the motivation of including strain effect on the interface.

For the methane adsorption, the interface was extended to three layers containing 354 atoms. This choice for the number of layers was considered as the best as it was not too large in terms of computational cost compared to using 5 layers yet the surface area was large enough to study multi-coverage adsorption of a few methane molecules. The z-direction was extended to at least 12 Å representing the vacuum region to avoid interaction with the neighboring cells with a 1 X 2 X 1 *k*-points. The adsorption of the methane molecule was studied at three different positions namely, the kaolinite-dominated part of the interface, the silica-dominated part, and the at the interface itself. Bader charge analysis [39,40] was carried out at the formation of the interface and also upon methane adsorption at the interface. The Quantum ATK virtual Nano lab was used for building the models and visualization of results [36,37] except for the Bader charge density difference which was visualized using VESTA [41].

For the classical Molecular Dynamics (MD) simulation using ReaxFF (Reactive Force Field), which can be used to study both reactive and non-reactive systems [42]. The choice of using ReaxFF was to save computational time compared to *Ab initio* Molecular Dynamics. This is especially because of the large number of atoms involved in this study. Moreover, ReaxFF could also give insights if new chemical bonds are formed compared to the conventional classical MD. The DFT optimized silica-kaolinite interface was used as the input file for the MD simulation. The CaSiAlO.ff, which was developed from studying clay-zeolite systems [43], was the force field used to study methane adsorption on the Silica-Kaolinite interface as it contained all the elements (C/H/O/Si/Al) in the studied system. The number of iterations for the system was 40,000 with a time step of 0.25 fs since the system contained hydrogen bonds making a totatl time of 10 ps. The NPT Berendsen method was used at 450 K and 500 bar with a damping constant of 100 fs and 500 fs for both temperature and pressure, respectively. The selected temperature and pressure correspond to the realistic conditions found in regional reservoirs [15]. The ADF input program version 2019.301, by Software for Chemistry and Materials (SCM), was used for visualizing and analyzing the results from the trajectory [44].

3. Results and discussion

3.1. Strain effect

In building the interface, the lattices of the two surfaces need to match; hence, a strain is applied to either surface or both surfaces. The two surfaces could be matched by either putting the strain on the silica surface alone or the kaolinite surface alone or both surfaces. However, a particular strain percentage is automatically calculated based on the lattice of both surfaces using the interface builder in Quantum ATK virtual nano lab builder. This method uses mathematical equations which are ingrained in the interface builder. The unit vectors of the two surfaces are extracted; the strain tensor from the unit cell of one surface is calculated using three different straining methods. The first method strains the silica surface only, while the second method strains the kaolinite surface only, while the third method strains both surfaces equally.

The ATK program calculates the optimum values of the strain. The detailed calculation methods are explained in the manual of the interface builder of Quantum ATK (https://docs.quantumatk.com/technicalnotes/interface_builder/interface_builder.html#interface-builder). Consequently, the optimum values of strain are determined for the silica, kaolinite and the combined surface as 4.8%, 4.3%, and 2.3%, respectively. These three possible strains would form an interface with a bonding system. After optimizing the three surfaces, the strained surface which showed the minimum total energy when strain applied only on Kaolinite surface, followed by the combined surface and finally the silica surface (see Table 1). Hence, the most stable interface of the silica-kaolinite system is obtained when the strain is applied on kaolinite surface only. It is important to reiterate that the bulk of each surface was optimized and thereafter cleaved at the 001 miller indices before being merged to create an interface. After the interface creation based on different strains applied then a second optimization was done to see which optimized interface based on the strain effect is the most stable (which in this case is 4.3%). Creating the interface first and thereafter cleaving the interface at 001 may lead to a different geometry which may be wrong, especially in a case where both surfaces do not have the same values for their most stable miller indices.

At the interface, the silicon (in silica) forms two bonds with the oxygen atoms in Kaolinite (Fig. 1), that is the interface is formed by the chemical bond of one silicon atom from the silica surface to two oxygen atoms from the kaolinite surface. The Bader charge density difference (Fig. 2) denotes the charge redistribution from the interface. It is calculated by subtracting the charge densities of both silica and kaolinite surfaces alone from the charge density of the silica-kaolinite interface. The electron densities can be seen in the yellow and blue lobes, which

Table 1
The effect of strain on the silica-kaolinite interface.

% Strain	4.8		4.3		2.3	
Surface	Silica	Kaolinite	Silica	Kaolinite	Silica	Kaolinite
Strain position	Silica		kaolinite		Both surfaces	
Total Energy (eV)	−846.440		−847.694		−847.068	

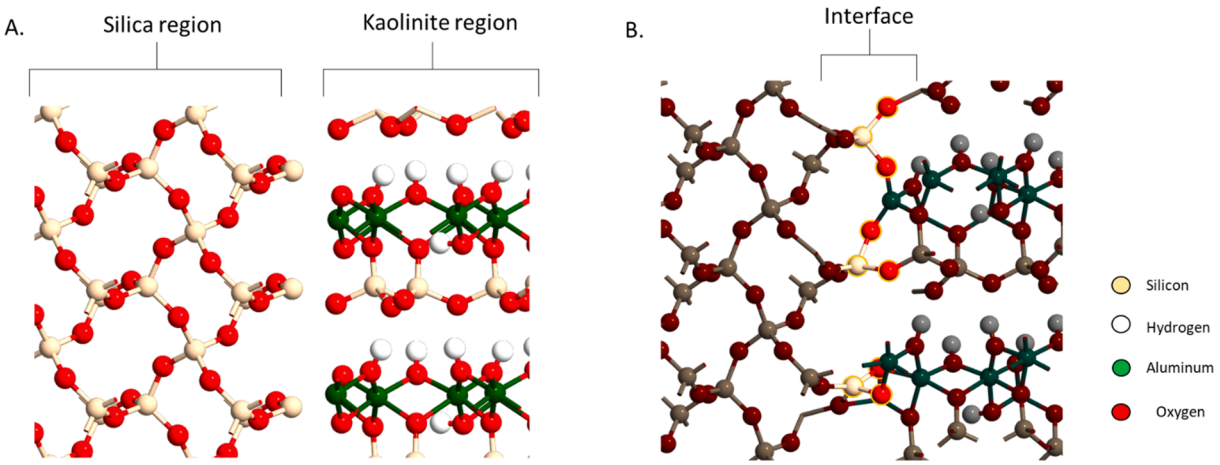

Fig. 1. The silica-kaolinite interface (a) before and (b) after optimization. The silica surface is on the left while the kaolinite surface is on the right. The highlighted atoms and bonds show where the two materials joined to form an interface.

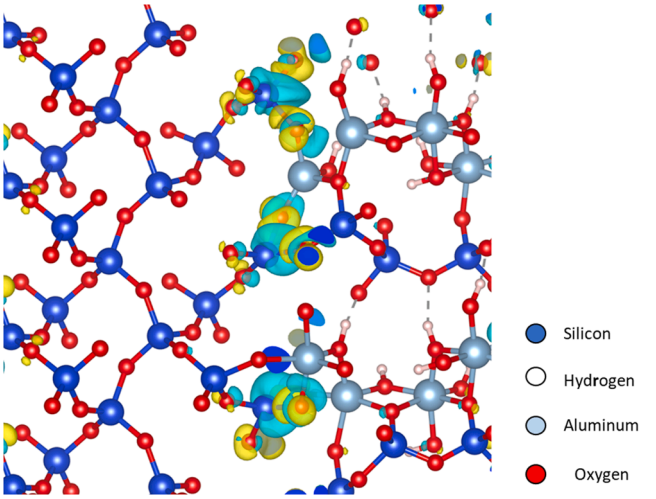

Fig. 2. The charge density difference at the silica-kaolinite interface. Yellow and blue colors represent the negative and positive electron density, respectively. The highlighted atoms and bonds show where the two materials joined to form an interface while the dashed line represents hydrogen bonding.

represent the negative and positive electron densities, respectively. The blue lobes could be seen around the silicon atom, while the yellow lobes are around the oxygen atoms. This confirms that oxygen is more electronegative than silicon; that is, oxygen donates its electrons to silicon to form the Si-O bonds.

3.2. Adsorption studies

DFT was used to understand the mode of adsorption of methane on the silica-kaolinite interface using Eq. (1). The methane molecule and three layers of the silica-kaolinite interface were optimized and their corresponding total energies E_{CH_4} and $E_{surface}$ of the isolated systems of methane and the interface (surface) alone were noted. The former was placed on three different positions of the latter, which is the silica dominated side, the interface (where silica joins with kaolinite), and the kaolinite dominated side (Fig. 3). The calculated adsorption energies showed that methane adsorbed stronger on the kaolinite region followed by the interface and then had the lowest adsorption at the silica region (Table 2). The results depicted that the mode of adsorption is physisorption (physical adsorption) because of the values of the adsorption energy. This result was in agreement with previous studies on methane adsorption on kaolinite system alone [45] and silica surfaces alone [46]. These studies were based on using different methods that is GCMC (Grand Canonical Monte Carlo) method for the kaolinite studies and small anlgle Neutron scattering method for the silica studies. Hence, the adsorption energy values cannot be easily compared. Nevertheless, the conclusion that the mode of adsorption of methane on kaolinite and silica is physisorption is agreed upon. Moreover, the adsorption energy of the silica region (-0.102 eV) was in close agreement to an earlier work (-0.13 eV) of ours using DFT which studied the adsorption of small molecules including methane on silica surface alone [47].

$$E_{ads.} = E_{surface+CH_4} - E_{surface} - E_{CH_4}$$

To ascertain the true nature of adsorption as a representative of the bulk, the number of layers of the interface was increased from three to five layers. However, the surface area was decreased this time to compliment the thickness. The five-layer interface (Fig. 4) contained 340 atoms which are similar to the number of atoms in the three layers earlier studied (354 atoms). The adsorption energies of methane on the five-layer interface were similar to those observed in three layers (Table 2) as the difference was within the range of ± 0.03 eV. Though the interface had the highest value (-0.131 eV) in the five layers compared to what was observed in the three layers, which had Kaolinite dominated region as the highest adsorption energy (-0.129 eV). These differences are negligible as in both cases the values between both the interface and kaolinite dominated region are close. Moreover, the silica dominated region had the lowest adsorption energy in both cases. Hence, the order of adsorption is Silica-dominated < Kaolinite-dominated ≅ interface.

3.3. Coverage effect

To provide a better understanding of the adsorption of methane, the coverage effect was studied by adding more methane molecules to the interface. Herein, the 3-layer interface was used as it had a large surface area and hence would allow for more methane molecules on its surface compared to the 5-layer. The adsorption energy, $E_{ads.coverage}$, upon addition of more methane is calculated using eq. (2) where n refers to the number of methane molecules added. The adsorption energy decreases steadily from 6 methane molecules and remained negative upon reaching full coverage of 14 molecules for the first monolayer (Table S1). This decrease in adsorption energy continues until reaching a plateau at 47 molecules which is the fourth layer (Fig. 5). However, to account for the effect of methane-methane interaction amongst the layers, the E_{layer}, was derived which is the total energy of all the layers of methane without the interface divided by N, where N is the total number

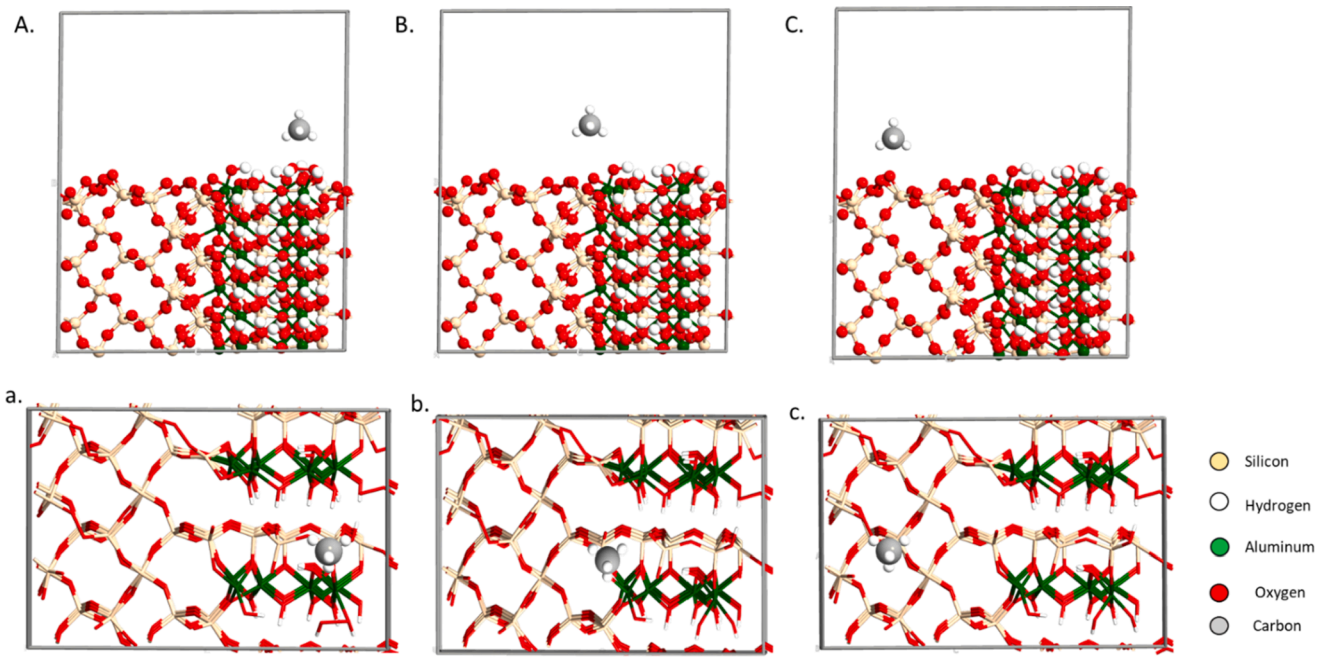

Fig. 3. The optimized structures of methane adsorbed on (A) Kaolinite-dominated interface (B) pure interface and (C) Silica-dominated interface. The top view corresponds to the small letters a, b, and c of each interface.

Table 2
Adsorption energies of methane at different positions on the interface.

No. of layers	3 Layers			
Position	$E_{surface}$	E_{CH_4}	$E_{surface+CH_4}$	$E_{ads.}(eV)$
Kaolinite dominated	−2461.411	−24.251	−2485.792	−0.129
Interface	−2461.411	−24.251	−2485.787	−0.124
Silica dominated	−2461.411	−24.251	−2485.765	−0.102
No. of layers	**5 layers**			
Interface	−2032.7551	−24.251	−2057.1408	−0.134
Kaolinite dominated	−2032.7551	−24.251	−2057.1376	−0.131
Silica dominated	−2032.7551	−24.251	−2057.0939	−0.087

of methane molecules in the four layers which in this case is 47 (eq. (3)).

Consequently, to get the adsorption energy for the fourth layer without the methane-methane interaction effect of other layers, the $E_{ads.layerenergy}$ term is coined from a modification of eq. (2) where the E_{layer}, is subtracted from the $E_{surface+nCH_4}$ (eq. (4)). Herein, n refers to the number of methane molecules (eq. (4)) in each layer which in the case of the fourth layer is 12. Hence, adsorption energy of 1.488 eV (Table 3) was obtained, which implied there was no longer adsorption as far as the fourth layer to the interface as compared to full coverage of the first layer (-0.559 eV). Hence, the negative adsorption energy value of −0.2 eV observed with 47 molecules is partly due to the methane-methane interaction and not the adsorption of methane to the interface.

$$E_{ads.coverage} = \frac{E_{surface+nCH_4} - E_{surface} - (n \times E_{CH_4})}{n} \quad (2)$$

$$E_{layer} = \frac{E_L}{N} \quad (3)$$

$$E_{ads.layerenergy} = \frac{\left[\left(E_{surface+nCH_4}\right) - E_{layer}\right] - \left[E_{surface} - (n \times E_{CH_4})\right]}{n} \quad (4)$$

3.4. Charge analysis

The Bader charge analysis was carried out to provide further insight into the nature of methane adsorption on the interface. To simplify this study, only the charge distribution of the methane molecule before and after adsorption was studied since the atoms on the interface are many (Fig. 6). The charge differences confirmed that the mode of adsorption is physisorption (Table 4) as the charge differences were not large enough to confirm the formation of a new chemical bond. Nevertheless, the carbon atom which is the center of mass of the methane molecule has the greatest charge difference when adsorbed on the kaolinite-dominated region of the interface. This observation correlates very well with what was reported earlier on the high adsorption energy on Kaolinite region.

3.5. Classical Molecular Dynamics analysis

Unlike DFT Molecular Dynamics (DFT-MD) which is computationally expensive, ReaxFF classical molecular dynamics (ReaxFF-MD) was carried out to confirm if there were no new chemical bonds formed between methane and the interface. Moreover, MD could be used to study more atoms than DFT and also at the operating conditions of the reservoir which are usually at high pressure and high temperature (HPHT) in this case, 450 K and 500 bar. The DFT optimized interface was used as the input slab for the MD simulation with 30 methane molecules put above the slab. The simulation which lasted for 10 ps was long enough to observe that no reactions were formed via ReaxFF. Hence, corroborating what was earlier observed that the mode of adsorption is physisorption.

Nevertheless, the radial distribution function (RDF) which defines the possibility of finding an atom at a distance r from another marked atom, which is calculated using the formula in eq. (5) [48,49]. Herein, the RDF of a Carbon atom, which is the center of mass of methane, is compared to both Aluminium and Silicon (Fig. 7a). It is important to note that when comparing the RDF of Carbon to Aluminium this represents comparing methane to the kaolinite-dominated region as the Carbon atom represents methane while Aluminium represents Aluminium which is only present in kaolinite. However, this cannot be said of the RDF of Carbon and Silicon as both kaolinite and silica contain silicon atoms. The RDF confirms that there are no chemical bonds formed in both C-Al and C-Si as the shortest pair distance is larger than 3 Å (Fig. 7a). The C-Al curve has two large peaks of which one coincides

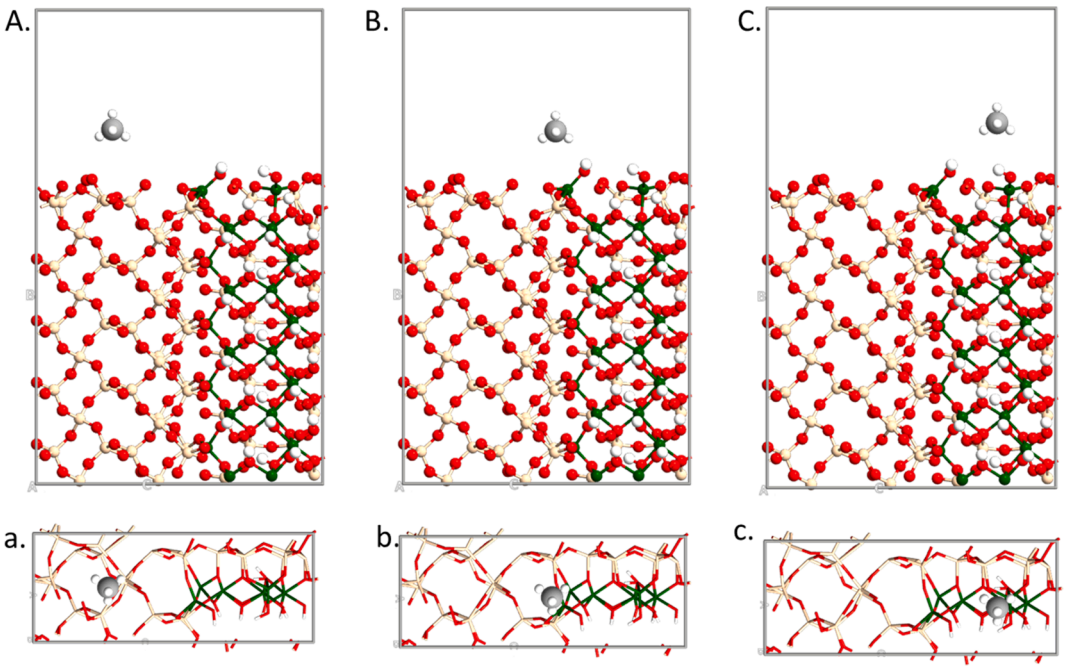

Fig. 4. The optimized 5-layer structures of (A) Kaolinite-dominated interface (B) pure interface and (C) Silica-dominated interface. The top view corresponds to the small letters a, b, and c of each interface.

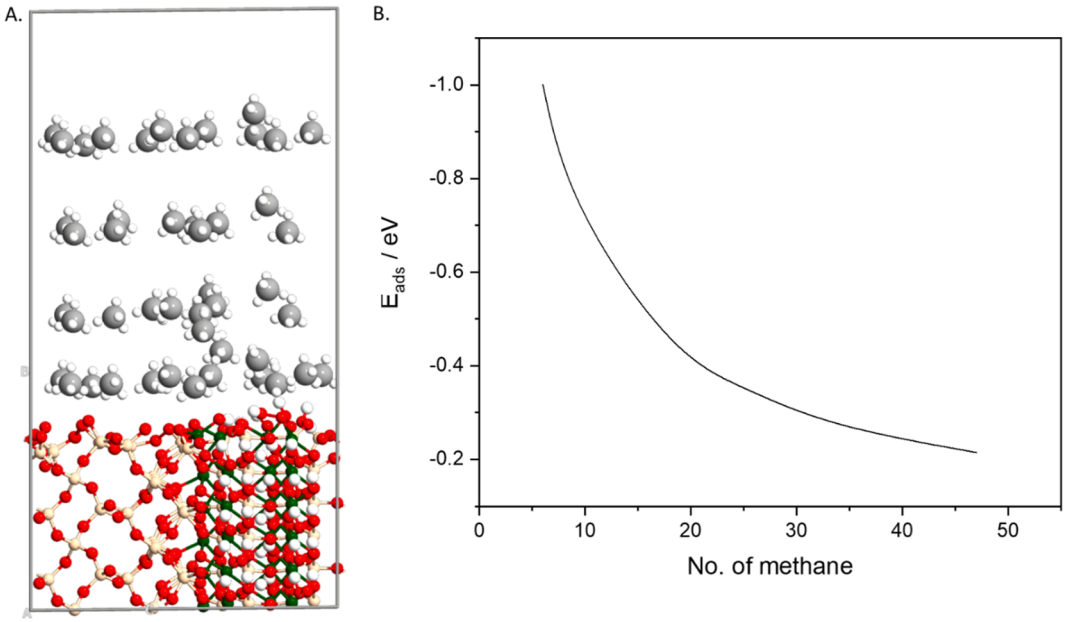

Fig. 5. The (a) optimized structure of 4 layers (47 molecules) of methane adsorbed on the interface and (b) the graph of adsorption energy against the number of methane molecules.

Table 3
Adsorption energies of multi coverage effect.

No. of CH_4in layer	Layer position	$E_{surface}$	E_{CH_4}	$E_{surface+CH_4}$	$E_{ads.}(eV)$
14	1st	−2461.411	−24.251	−2808.76	−0.559
12	4th	−2461.411	−24.251	−2758.87	1.488*

* The $E_{ads.}$ value here is the $E_{ads.layerenergy}$ in the case of the 4th layer.

with C-Si at around 5 Å while the other is around 7 Å.

Hence, to understand which region would mostly adsorb the methane molecules, the RDF of two methane molecules, which are at the interface (Fig. 8), are observed for the carbon atom. These carbons are selected as one of the methane molecules (C-72) from the silica dominated region (Si-1009) and the other from the kaolinite dominated (Al-13). The RDF of C_{72}-Al_{13} showed a large peak for C_{72}-Al_{13} at 3.6 Å and comes to a plateau at 7.5 Å compared to C_{72}-Si_{1009} which had a smaller peak at 6 Å and reached a plateau at 11 Å (Fig. 7b). This confirmed what was earlier observed in DFT studies that methane is more adsorbed on the kaolinite dominated region than the silica dominated region.

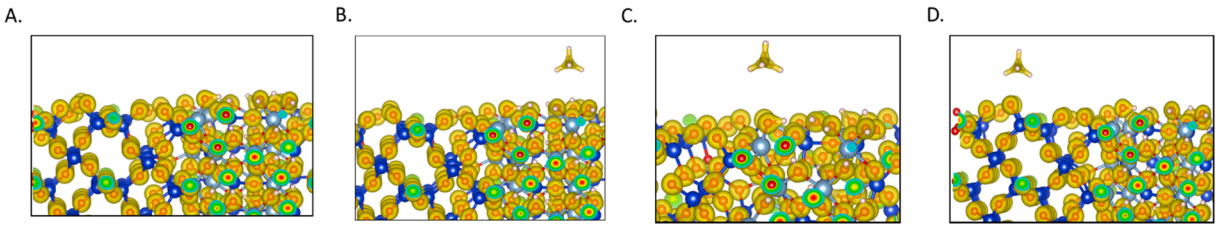

Fig. 6. The BADER charge densities before (A) and after methane adsorption at the (B) Kaolinite-dominated interface (C) pure interface and (D) Silica-dominated interface.

Table 4
Bader charge analysis of methane adsorption on the interface.

		After methane adsorption			Charge difference		
Atom	Before Adsorption	Kaolinite Dominated	Interface	Silica Dominated	Kaolinite Dominated	Interface	Silica Dominated
C	4.467	4.181	4.325	4.274	−0.286	−0.142	−0.193
H1	0.914	1.039	0.957	0.988	0.125	0.043	0.074
H2	0.931	0.912	0.891	0.973	−0.018	−0.040	0.043
H3	0.845	0.909	0.907	0.916	0.064	0.062	0.071
H4	0.843	0.957	0.922	0.839	0.114	0.079	−0.004

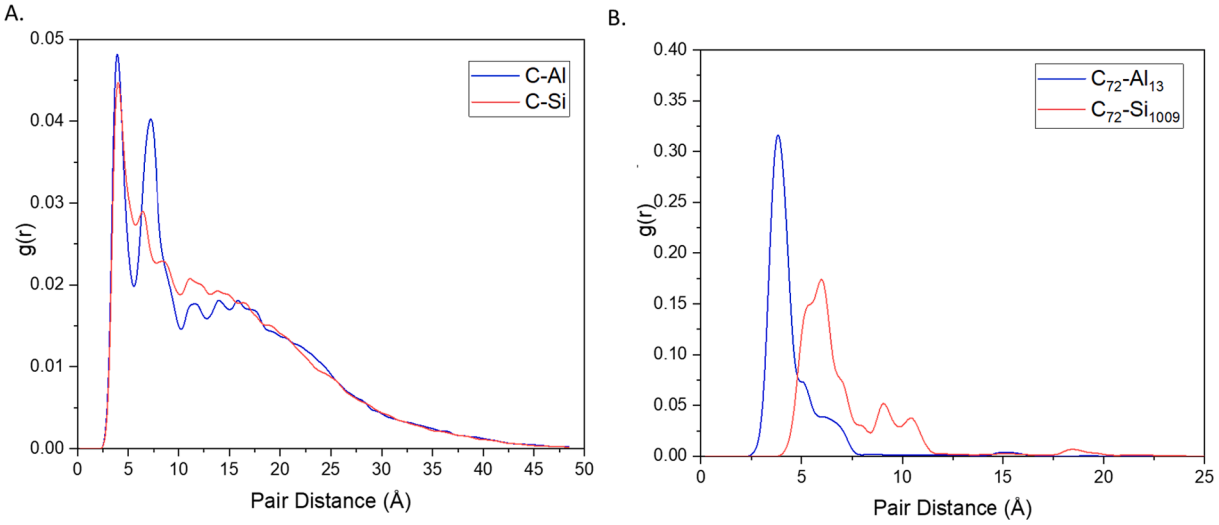

Fig. 7. The radial distribution function (RDF) curve of (A) all carbon atoms (methane) to all Aluminum and Silicon atoms (B) Carbon-72 (methane) to Aluminium-13 (Kaolinite) and Silicon-1009 (Silica).

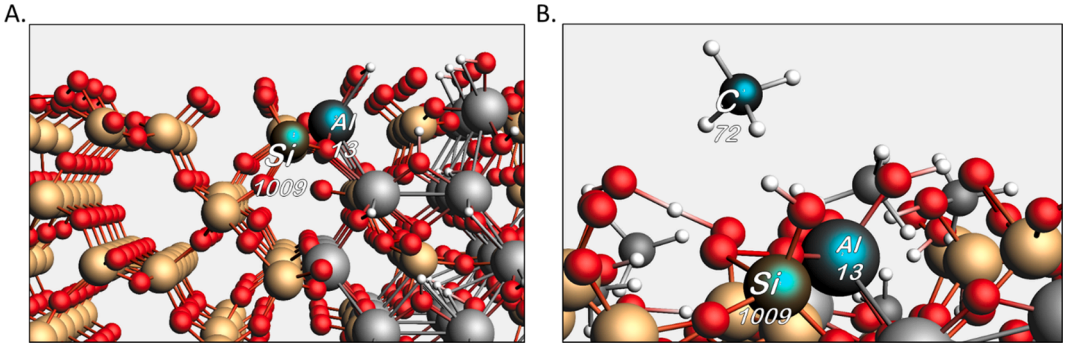

Fig. 8. The positions of (A) Aluminium-13 (Kaolinite) and Silicon-1009 (Silica) at the start and (B) Carbon-72 (methane), Aluminium-13 (Kaolinite), and Silicon-1009 (Silica) at the end of the molecular dynamics simulation.

$$\rho(r) = \rho^{bulk} g(r) \quad (5)$$

4. Conclusion

Molecular simulation techniques including DFT and MD were used to study the adsorption of methane on a silica-kaolinite interface. Whilst building the interface, strain effect was considered between the two initial surfaces of silica and kaolinite, respectively. Applying the strain on the kaolinite surface had the most stable silica-kaolinite interface as opposed to applying the strain on the silica surface alone or on both surfaces equally. The adsorption of methane was studied at three different positions- at the silica dominated region, at the kaolinite dominated region and at the interface where the two surfaces merge. The mode of adsorption of methane in all three positions is physisorption. However, the kaolinite dominated region has a stronger adsorption than the silica-dominated region. The charge analysis and ReaxFF MD study confirmed that no new chemical bonds are formed hence corroborating that the mode of adsorption is physisorption. The coverage effect showed that methane adsorption decreased from −0.559 eV (first layer) and reached a plateau at −0.215 eV (fourth layer). However, methane-methane interaction between the layers of methane contributes to the negative adsorption energy observed in the coverage effect and is suggested to be responsible for the negative value observed when the fourth layer of methane is considered. The RDF analysis supported that methane is preferentially adsorbed on the kaolinite dominated region than silica dominated region. The following conclusions were derived from this study:

1. Applying a strain of 4.3% on kaolinite would lead to the most stable silica-kaolinite interface.
2. The mode of adsorption of methane on the silica-kaolinite interface is physisorption
3. The order of adsorption methane adsorption on the silica-kaolinite interface is Silica-dominated region < Kaolinite-dominated region ≅ interface.
4. The coverage effect showed that methane adsorption decreased from −0.559 eV (first layer) and reached a plateau at −0.215 eV (fourth layer). However, methane-methane interaction between the methane layers contributes to the negative adsorption energy observed when the coverage effect reached four layers of methane.
5. The charge analysis verified that the mode of adsorption is physical adsorption and kaolinite dominated region has greater adsorption than silica dominated region
6. ReaxFF MD analysis at HPHT confirmed that no reactions are formed between methane and the interface.
7. The RDF analysis confirmed that methane is preferentially adsorbed on the kaolinite dominated region than silica dominated region.

CRediT authorship contribution statement

Abdulmujeeb T. Onawole: Conceptualization, Data curation, Methodology, Writing - original draft. **Mustafa S. Nasser:** Conceptualization, Funding acquisition, Writing - original draft. **Ibnelwaleed A. Hussein:** Methodology, Conceptualization, Data curation, Methodology, Writing - original draft. **Mohammed J. Al-Marri:** Funding acquisition, Conceptualization, Writing - original draft. **Santiago Aparicio:** Conceptualization, Methodology.

Declaration of Competing Interest

The authors declare that they have no known competing financial interests or personal relationships that could have appeared to influence the work reported in this paper.

Acknowledgment

This work was supported by funding # NPRP12S-0130-190023 from Qatar National Research Fund. The Research Computing group at Texas A&M University at Qatar (funded by Qatar Foundation) provided the HPC facilities used in this work. Qatar University and the Gas Processing Center are acknowledged for their support. The outcomes attained herein are exclusively the responsibility of the authors. The publication of this article was funded by the Qatar National Library.

Appendix A. Supplementary data

Supplementary data to this article can be found online at https://doi.org/10.1016/j.apsusc.2021.149164.

References

[1] Q. Wang, R. Li, Research status of shale gas: A review, Renew. Sustain. Energy Rev. 74 (2017) 715–720, https://doi.org/10.1016/j.rser.2017.03.007.
[2] S. Rani, E. Padmanabhan, B.K. Prusty, Review of gas adsorption in shales for enhanced methane recovery and CO2 storage, J. Pet. Sci. Eng. 175 (2019) 634–643, https://doi.org/10.1016/j.petrol.2018.12.081.
[3] Y. Gensterblum, A. Ghanizadeh, R.J. Cuss, A. Amann-Hildenbrand, B.M. Krooss, C. R. Clarkson, J.F. Harrington, M.D. Zoback, Gas transport and storage capacity in shale gas reservoirs - A review, Part A: Transport processes, J. Unconv. Oil Gas Resour. 12 (2015) 87–122, https://doi.org/10.1016/j.juogr.2015.08.001.
[4] S.A. Solarin, L.A. Gil-Alana, C. Lafuente, An investigation of long range reliance on shale oil and shale gas production in the U.S. market, Energy. 195 (2020), 116933, https://doi.org/10.1016/j.energy.2020.116933.
[5] C. Avraam, D. Chu, S. Siddiqui, Natural gas infrastructure development in North America under integrated markets, Energy Policy. 147 (2020), 111757, https://doi.org/10.1016/j.enpol.2020.111757.
[6] B. Fattouh, H.V. Rogers, P. Stewart, The US shale gas revolution and its impact on Qatar's position in gas markets, Columbia University in the City of New York, 2015.
[7] X. Tong, G. Zhang, Z. Wang, Z. Wen, Z. Tian, H. Wang, F. Ma, Y. Wu, Distribution and potential of global oil and gas resources, Pet. Explor. Dev. 45 (2018) 779–789, https://doi.org/10.1016/S1876-3804(18)30081-8.
[8] M. Voltolini, H.R. Wenk, N.H. Mondol, K. Bjørlykke, J. Jahren, Anisotropy of experimentally compressed kaolinite-illite-quartz mixtures, Geophysics. 74 (2009) D13–D23, https://doi.org/10.1190/1.3002557.
[9] S. Tian, V. Erastova, S. Lu, H.C. Greenwell, T.R. Underwood, H. Xue, F. Zeng, G. Chen, C. Wu, R. Zhao, Understanding Model Crude Oil Component Interactions on Kaolinite Silicate and Aluminol Surfaces: Toward Improved Understanding of Shale Oil Recovery, Energy and Fuels. 32 (2018) 1155–1165, https://doi.org/10.1021/acs.energyfuels.7b02763.
[10] H. Wang, L. Chen, Z. Qu, Y. Yin, Q. Kang, B. Yu, W.Q. Tao, Modeling of multi-scale transport phenomena in shale gas production — A critical review, Appl. Energy. 262 (2020), https://doi.org/10.1016/j.apenergy.2020.114575.
[11] S. Duan, M. Gu, M. Tao, X. Xian, Adsorption of Methane on Shale: Statistical Physics Model and Site Energy Distribution Studies, Energy and Fuels. 34 (2020) 304–318, https://doi.org/10.1021/acs.energyfuels.9b03746.
[12] G. Feng, Y. Zhu, S. Chen, Y. Wang, W. Ju, Y. Hu, Z. You, G.G.X. Wang, Supercritical Methane Adsorption on Shale over Wide Pressure and Temperature Ranges: Implications for Gas-in-Place Estimation, ACS Appl. Mater. Interfaces. (2020), https://doi.org/10.1021/acs.energyfuels.9b04498.
[13] T.Y. Wang, S.C. Tian, Q.L. Liu, G.S. Li, M. Sheng, W.X. Ren, P.P. Zhang, Pore structure characterization and its effect on methane adsorption in shale kerogen, Pet. Sci. (2020), https://doi.org/10.1007/s12182-020-00528-9.
[14] Z. Gao, B. Li, J. Li, Y. Zhang, C. Ren, B. Wang, Study on the Adsorption and Thermodynamic Characteristics of Methane under High Temperature and Pressure, Energy & Fuels. (2020), https://doi.org/10.1021/acs.energyfuels.0c02584.
[15] A. Al Siddiqi, R.A. Dawe, A Review Of Petroleum Engineering Aspects Of Qatar's Oil And Gas, Eng. J. Univ. Qatar. 11 (1998) 11–45.
[16] G. Carchini, M.J. Al-marri, I.A. Hussein, S. Aparicio, Ab Initio Molecular Dynamics Investigation of CH 4 /CO 2 Adsorption on Calcite: Improving the Enhanced Gas Recovery Process, ACS, Omega. (2020), https://doi.org/10.1021/acsomega.0c04694.
[17] L.O. Lawal, T. Olayiwola, S. Abdel-Azeim, M. Mahmoud, A.O. Onawole, M. S. Kamal, Molecular simulation of kerogen-water interaction: Theoretical insights into maturity, J. Mol. Liq. 299 (2020), 112224, https://doi.org/10.1016/j.molliq.2019.112224.
[18] B. Zhang, J. Kang, T. Kang, Effect of water on methane adsorption on the kaolinite (0 0 1) surface based on molecular simulations, Appl. Surf. Sci. 439 (2018) 792–800, https://doi.org/10.1016/j.apsusc.2017.12.239.
[19] J. Zhao, J.M. Wang, X.Z. Qin, W.S. Han, Z.G. Tao, M.C. He, First-principles calculations of methane adsorption at different coverage on the kaolinite (001) surface, Mater. Today Commun. 18 (2019) 199–205, https://doi.org/10.1016/j.mtcomm.2018.12.011.

[20] J. Zhao, Z. Wang, P. Guo, Q. Luo, Molecular level investigation of methane and carbon dioxide adsorption on SiO2 surface, Comput. Mater. Sci. 168 (2019) 213–220, https://doi.org/10.1016/j.commatsci.2019.05.044.
[21] K. Lin, Q. Yuan, Y.P. Zhao, C. Cheng, Which is the most efficient candidate for the recovery of confined methane: Water, carbon dioxide or nitrogen? Extrem. Mech. Lett. 9 (2016) 127–138, https://doi.org/10.1016/j.eml.2016.05.014.
[22] K. Lin, Q. Yuan, Y. Zhao, Using graphene to simplify the adsorption of methane on shale in MD simulations, Comput. Mater. Sci. 133 (2017) 99–107, https://doi.org/10.1016/j.commatsci.2017.03.010.
[23] K. Lin, X. Huang, Y.P. Zhao, Combining Image Recognition and Simulation to Reproduce the Adsorption/Desorption Behaviors of Shale Gas, Energy and Fuels. 34 (2020) 258–269, https://doi.org/10.1021/acs.energyfuels.9b03669.
[24] G. Kresse, J. Furthmüller, Efficient iterative schemes for ab initio total-energy calculations using a plane-wave basis set, Phys. Rev. B - Condens. Matter Mater. Phys. 54 (1996) 11169–11186, https://doi.org/10.1103/PhysRevB.54.11169.
[25] L.M. Yang, E. Ganz, S. Svelle, M. Tilset, Computational exploration of newly synthesized zirconium metal-organic frameworks UiO-66, -67, -68 and analogues, J. Mater. Chem. C. 2 (2014) 7111–7125, https://doi.org/10.1039/c4tc00902a.
[26] J.P. Perdew, K. Burke, M. Ernzerhof, Generalized gradient approximation made simple, Phys. Rev. Lett. 77 (1996) 3865–3868, https://doi.org/10.1103/PhysRevLett.77.3865.
[27] G. Kresse, D. Joubert, From ultrasoft pseudopotentials to the projector augmented-wave method, Phys. Rev. B. 59 (1999) 1758–1775, https://doi.org/10.1103/PhysRevB.59.1758.
[28] P.E. Blöchl, Generalized separable potentials for electronic-structure calculations, Phys. Rev. B. 41 (1990) 5414–5416, https://doi.org/10.1103/PhysRevB.41.5414.
[29] J.B.A. Davis, F. Baletto, R.L. Johnston, The Effect of Dispersion Correction on the Adsorption of CO on Metallic Nanoparticles, J. Phys. Chem. A. 119 (2015) 9703–9709, https://doi.org/10.1021/acs.jpca.5b05710.
[30] S. Grimme, J. Antony, S. Ehrlich, H. Krieg, A consistent and accurate ab initio parametrization of density functional dispersion correction (DFT-D) for the 94 elements H-Pu, J. Chem. Phys. 132 (2010), https://doi.org/10.1063/1.3382344.
[31] K. Persson, Materials Data on SiO2 (SG:152), by Materials Project (2014), https://doi.org/10.17188/1272685.
[32] K. Persson, Materials Data on Al2Si2H4O9 (SG:1), by Materials Project (2014), https://doi.org/10.17188/1264975.
[33] A. Jain, S.P. Ong, G. Hautier, W. Chen, W.D. Richards, S. Dacek, S. Cholia, D. Gunter, D. Skinner, G. Ceder, K.A. Persson, Commentary: The Materials Project: A materials genome approach to accelerating materials innovation, APL Mater. 1 (2013), 011002, https://doi.org/10.1063/1.4812323.
[34] O.I. Malyi, V.V. Kulish, C. Persson, In search of new reconstructions of (001) α-quartz surface: A first principles study, RSC Adv. 4 (2014) 55599–55603, https://doi.org/10.1039/c4ra10726h.
[35] F. Fang, F. Min, L. Liu, J. Chen, B. Ren, C. Liu, Adsorption of Al(OH)n(3-n)+ (n = 2–4) on Kaolinite (001) Surfaces: A DFT study, Appl. Clay Sci. 187 (2020), https://doi.org/10.1016/j.clay.2020.105455.
[36] S. Smidstrup, T. Markussen, P. Vancraeyveld, J. Wellendorff, J. Schneider, T. Gunst, B. Verstichel, D. Stradi, P.A. Khomyakov, U.G. Vej-Hansen, M.-E. Lee, S. T. Chill, F. Rasmussen, G. Penazzi, F. Corsetti, A. Ojanperä, K. Jensen, M.L. N. Palsgaard, U. Martinez, A. Blom, M. Brandbyge, K. Stokbro, QuantumATK: an integrated platform of electronic and atomic-scale modelling tools, J. Phys. Condens. Matter. 32 (2020) 1–36, https://doi.org/10.1088/1361-648x/ab4007.
[37] A.T. Onawole, I.A. Hussein, Effect of surface morphology on methane interaction with calcite : a DFT study, RSC Adv. 10 (2020) 16669–16674, https://doi.org/10.1039/D0RA02471F.
[38] E. Elbashier, I. Hussein, G. Carchini, A. Sakhaee Pour, G.R. Berdiyorov, Effect of strain on gas adsorption in tight gas carbonates: A DFT study, Comput. Mater. Sci. (2020), 110186, https://doi.org/10.1016/j.commatsci.2020.110186.
[39] R.F.W. Bader, Atoms in molecules, Acc. Chem. Res. 18 (1985) 9–15.
[40] G. Henkelman, A. Arnaldsson, H. Jónsson, A fast and robust algorithm for Bader decomposition of charge density, Comput. Mater. Sci. 36 (2006) 354–360, https://doi.org/10.1016/j.commatsci.2005.04.010.
[41] K. Momma, F. Izumi, VESTA 3 for three-dimensional visualization of crystal, volumetric and morphology data, J. Appl. Crystallogr. 44 (2011) 1272–1276, https://doi.org/10.1107/S0021889811038970.
[42] A. Rahnamoun, M.C. Kaymak, M. Manathunga, A.W. Götz, A.C.T. van Duin, K. M. Merz, H.M. Aktulga, ReaxFF/AMBER—A Framework for Hybrid Reactive/Nonreactive Force Field Molecular Dynamics Simulations, J. Chem. Theory Comput. (2020), https://doi.org/10.1021/acs.jctc.0c00874.
[43] M.C. Pitman, A.C.T. Van Duin, Dynamics of confined reactive water in smectite clay-zeolite composites, J. Am. Chem. Soc. 134 (2012) 3042–3053, https://doi.org/10.1021/ja208894m.
[44] G. te Velde, F.M. Bickelhaupt, E.J. Baerends, C. Fonseca Guerra, S.J.A. van Gisbergen, J.G. Snijders, T. Ziegler, Chemistry with ADF, J. Comput. Chem. 22 (2001) 931–967, https://doi.org/10.1002/jcc.1056.
[45] J. Xiong, X. Liu, L. Liang, Q. Zeng, Adsorption Behavior of Methane on Kaolinite, Ind. Eng. Chem. Res. 56 (2017) 6229–6238, https://doi.org/10.1021/acs.iecr.7b00838.
[46] W.S. Chiang, E. Fratini, P. Baglioni, J.H. Chen, Y. Liu, Pore Size Effect on Methane Adsorption in Mesoporous Silica Materials Studied by Small-Angle Neutron Scattering, Langmuir. 32 (2016) 8849–8857, https://doi.org/10.1021/acs.langmuir.6b02291.
[47] G. Carchini, I. Hussein, M.J. Al-Marri, R. Shawabkeh, M. Mahmoud, S. Aparicio, A theoretical study of gas adsorption on α-quartz (0 0 1) for CO2 enhanced natural gas recovery, Appl. Surf. Sci. 525 (2020), 146472, https://doi.org/10.1016/j.apsusc.2020.146472.
[48] D. Chandler, Introduction to modern statistical mechanics, Introd. to Mod. Stat. Mech. by David Chandler, Pp. 288. Foreword by David Chandler. Oxford Univ. Press. Sep 1987. ISBN-10 0195042778. ISBN-13 9780195042771. (1987) 288.
[49] A.T. Onawole, I.A. Hussein, M.E.M. Ahmed, M.A. Saad, S. Aparicio, Ab Initio molecular dynamics of the dissolution of oilfield pyrite scale using borax, J. Mol. Liq. 302 (2020) 1–10.